High-Speed and High-Resolution Interrogation of a Strain and Temperature Random Grating Sensor

Hong Deng, *Student Member, IEEE*, Ping Lu , Stephen J. Mihailov , *Member, IEEE*, and Jianping Yao , *Fellow, IEEE, Fellow, OSA*

Abstract—High-speed and high-resolution interrogation of a random fiber grating sensor based on spectral shaping and wavelength-to-time (SS-WTT) mapping, and pulse compression for simultaneous measurement of strain and temperature is proposed and demonstrated. In the proposed system, an ultrashort pulse is spectrum shaped by a high-birefringence (Hi-Bi) random grating (HBRG) to generate two orthogonally polarized spectra with a wavelength difference determined by the birefringence of the HBRG, which are then fed to a dispersive optical loop in which a linearly chirped fiber Bragg grating (LCFBG) is incorporated, to perform linear WTT mapping, to generate two temporally separated optical pulses, which are converted to two random electrical waveforms at a photodetector). Random pulse compression is then performed to increase the interrogation resolution. By measuring the time shifts of the temporally compressed pulses, the strain and temperature information is retrieved. An experiment is performed. The experimental results show that the proposed random grating sensor and its interrogation system can provide a strain and temperature resolution of 7.1 $\mu\varepsilon$ and 0.79 °C at an ultrahigh speed of 20 MHz.

Index Terms—Fiber Bragg grating, interrogation, sensor, linearly chirped fiber Bragg grating.

I. INTRODUCTION

FIBER grating sensors, with intrinsic advantages such as light weight, compact size, immunity to electromagnetic interference (EMI), and high tolerance to harsh environment, have been extensively investigate and have found numerous applications in areas such as in aerospace engineering, civil engineering, petrochemical industry, and medical care [1]–[3]. Usually, a fiber grating sensor is interrogated by an optical spectrum analyzer (OSA) to monitor its wavelength shift, but the interrogation speed is slow, especially when the sensing resolution is high [4].

To increase the interrogation speed while maintaining a high resolution, various interrogation techniques have been proposed.

For example, using a bulky dispersive element to convert the wavelength information to its spatial light distribution and using a linear-array detector to detect the spatial light distribution, the wavelength information can be measured in real time [5]. The system in [5] is simple and stable, but the free-space implementation makes the system relatively bulky and costly. The use of an optical edge filter [6], [7] to convert the wavelength shift to an intensity change is another approach that can provide real time interrogation. The major limitation of using an edge filter is the power variations of the light source, which would be translated to intensity changes, making the interrogation accuracy reduced. To increase the accuracy, we may use an optical interferometric scanner to covert the wavelength shift to an optical phase shift, with the phase shift estimated by a lock-in amplifier [8]. The measurement resolution is significantly improved, but the stability is poor due to the use of an interferometer which is extremely sensitive to environmental changes.

Recently, fiber Bragg grating (FBG) sensors interrogated based on microwave photonics (MWP) techniques have been proposed. The key advantages of using MWP techniques are the ultra-high interrogation speed and high resolution, which are realized by translating the wavelength shift in the optical domain to a microwave frequency change in the electrical domain. The microwave frequency change can be measured using a digital signal processor (DSP) at an ultra-high speed and resolution. For example, in [9] two FBGs with one serving as a sensor FBG and the other as a reference FBG were used to slice the spectrum of an ultrashort pulse, to generate two spectrums. By wavelength-to-time mapping [10], [11], [12], the two spectrums were converted to two temporal pulses. The sensing information is obtained by measuring the frequency of the temporal interference pattern, with an increased resolution. To further increase the measurement resolution, a linearly chirped microwave waveform was generated and used in the interrogation system [13]. By performing pulse compression, the resolution can be further increased. A similar approach using pulse compression was recently reported in [14], where a linearly chirped microwave waveform was filtered by a microwave photonic filter implemented using a phase-shifted FBG (PS-FBG). Again, by using pulse compression, the sensing resolution was improved. In [15], an optical chirped pulse is sent to two chirped FBGs, with one as a sensor FBG and the other as a reference FBG. Two time-delayed optical chirped pulses are obtained. By beating the two optical pulses at a photodetector (PD), a de-chirped microwave signal with its frequency corresponding to the time

delay difference between the two optical pulses was generated. Since the time delay difference is temperature or strain dependent, the frequency information reveals the sensing information. High precision interrogation can also be done using an optoelectronic oscillator (OEO) [16], [17]. For example, by using a PS-FBG in an OEO, a microwave signal with its frequency corresponding to the wavelength difference between the optical carrier wavelength and the notch wavelength can be generated. By monitoring the microwave frequency change, high speed and ultra-high resolution interrogation can be achieved. All the approaches reported in [9], [13]–[16] can provide high-speed and high-resolution interrogation. However, since interferometric structures are employed in the systems, the stability is poor.

In this paper, we propose an approach to implement high-speed and high-resolution interrogation of a random grating sensor without using an interferometric structure. The key component is a high-birefringence random grating (HBRG) sensor, which is fabricated in a polarization maintaining fiber (PMF) by pseudo-randomly varying the grating periods, providing a random reflection response. An ultra-short pulse from a mode-lock laser (MLL) is spectrum shaped by the HBRG to generate two random spectrums with the wavelength spacing determined by the birefringence of the HBRG, which are then fed to an optical loop in which a linearly chirped fiber Bragg grating (LCFBG) is incorporated. Linear wavelength-to-time mapping is implemented at the LCFBG in a complementary manner to generate two temporally separated random waveforms, corresponding to the spectrums along two orthogonal polarization directions. Using pulse compression, the temporal locations of the two random waveforms can be precisely measured, and thus the strain and temperature information can be retrieved. Because of the high randomness of the reflection spectral response of the HBRG, the compressed pulses are very narrow, leading to a significantly increased interrogation resolution. Furthermore, using the LCFBG in a complementary manner can provide complementary optical dispersion to the two orthogonally polarized spectrums. Thus, the two wavelength-to-time mapped temporal waveforms would experience positive and negative time delays, which would make the two temporal waveforms shift in the opposite directions, avoiding the overlap of the two random waveforms in the interrogation. In addition, without using an interferometric structure, the system is ultra-stable. The proposed approach is experimentally evaluated. Experimental results show that a strain and temperature resolution of 7.1 $\mu\varepsilon$ and 0.79 °C at an ultra-high speed of 20 MHz are achieved.

II. PRINCIPLE

The proposed interrogation system is shown in Fig. 1. An ultrashort optical pulse generated by a mode-locked laser (MLL) is sent through a bandpass optical filter and an optical circulator (OC1) to an HBRG serving as a sensor. A polarization controller (PC1) is used to control the polarization direction of the ultra-short pulse to have an angle of 45° relative to one principle axis of the HBRG. Thus, the incident light pulse is projected equally to the two principle axes of the HBRG. Two orthogonally polarized spectrums with a wavelength spacing determined by the
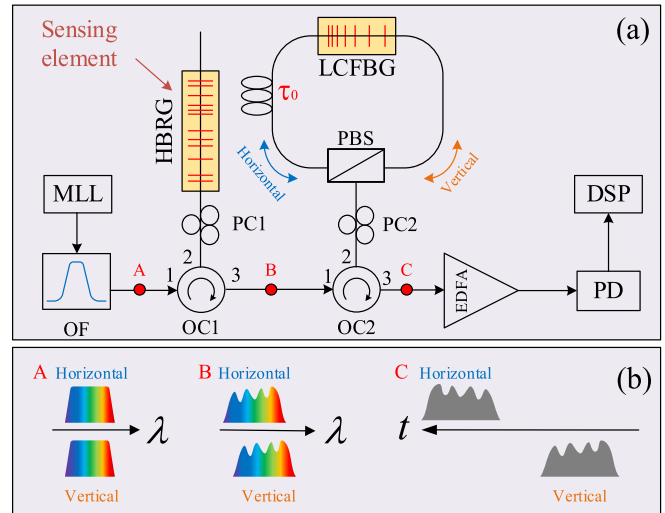

Fig. 1. (a) Schematic of the proposed HBRG sensor interrogation system; (b) the spectrums and temporal waveforms at different locations of the system. MLL: mode-locked laser; OC: optical circulator; PC: polarization controller; HBRG: high birefringence random grating; PBS: polarization beam splitter; LCFBG: linearly chirped fiber Bragg grating; EDFA: erbium-doped fiber amplifier; PD: photodetector; DSP: digital signal processor.

birefringence of the HBRG are generated and sent to an optical loop via a second OC (OC2) and a second PC (PC2). The optical loop consists of a polarization beam splitter (PBS), an LCFBG, and a delay line. PC2 is used to align the polarization directions of the optical pulses (horizontal and vertical) with the principle axes of the PBS, so that one optical pulse with its polarization aligned with one principle axis (say, horizontal) is directed to the left path, and the optical pulse with its polarization aligned with the vertical principle axis of the PBS (vertical) is directed to the right path. Then, the horizontally polarized light is reflected from the shorter wavelength end of the LCFBG, thus wavelength-to-time mapping is implemented at the LCFBG with a positive dispersion coefficient. Meanwhile, the vertically polarized light is reflected from the longer wavelength end, and wavelength-to-time mapping with a negative dispersion coefficient is implemented. The leaked light due to the imperfect reflection of the LCFBG is blocked by the PBS because of the orthogonal polarization. A section of single-mode fiber (SMF) is added to the left path to introduce an additional time delay, say τ_0, thus the reflected horizontally polarized pulse would experience a $2\tau_0$ extra time delay, to make the two pulses further separated in the time domain to avoid overlap. The two mapped optical pulses are then amplified by an erbium-doped fiber amplifier (EDFA) before photodetection at a PD, and two electrical random waveforms are generated, corresponding to the two random spectrums of the HBRG sensor. By performing pulse compression using a DSP, the two pulses are significantly compressed, which leads to a precise measurement of the temporal shifts of the two random waveforms, leading to an accurate retrieval of the strain and temperature information.

The key component of the generation system is the random grating. The random grating is fabricated based on the plane-by-plane writing technique using a Femto-second (fs) laser, which
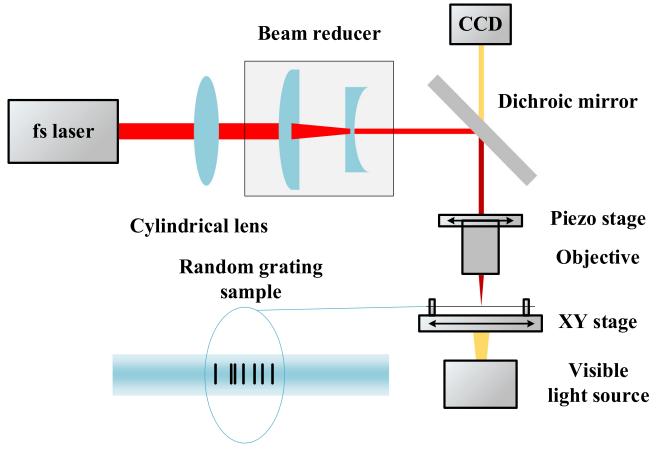
Fig. 2. Schematic of the setup for plane-by-plane grating fabrication [18]. fs laser: femtosecond laser.

is shown in Fig. 2 [18]. By using a microscope objective, pulses from the fs laser are focused to the fiber core region and make high localized changes to the refractive index of the fiber core. The objective is fixed on a translation stage driven by a piezo position system, which allows the focus to dither along the fiber axis. By randomly varying the grating planes spacing between 0 μm and 3.5 μm plane-by-plane, a random index modification is realized, leading to a random grating, and the spacing randomness is determined by a random number generated by a computer.

For a random grating, the core-core mode Fabry-Pérot interferences and core-cladding mode Mach-Zehnder interferences existing in the fiber would generate irregular reflections, leading to a random reflection spectrum. Because the transmitted core mode is much higher than the other modes, the spectrum of the transmitted light is almost the same as that of the incident light, with some loss [19]. By feeding a broadband light pulse into the random grating, a light pulse with a random spectrum can be reflected. The change of the environmental temperature and the applied strain will cause change in the interferometer length and effective refractive indices of the core mode and cladding modes, leading to a spectral shift in the corresponding reflection spectrum of the random grating.

Mathematically, the wavelength shift can be expressed as

$$\Delta\lambda = g_1\Delta\varepsilon + g_2\Delta T \qquad (1)$$

where $\Delta\varepsilon$ is the strain change, ΔT is the temperature change and g_1, g_2 are the corresponding coefficients, respectively.

Because the random spectrum is broad, direct interrogation of the spectrum shift using an optical spectrum analyzer (OSA) will have poor accuracy and low resolution. To increase the resolution, pulse compression technique can be employed. A random waveform can be compressed significantly by correlation [20]. If a shifted spectrum is correlated with a reference spectrum (a spectrum without experiencing a temperature or strain change), the correlation peak will appear at a location representing the spectrum shift. Thus, the shift of the spectrum can be accurately measured. However, the measurement of the spectrums using an OSA has a low speed. In the proposed approach, we convert

the spectrums to the time domain based on wavelength-to-time mapping, and the measurement can be done in the time domain using a high-speed DSP.

As shown in Fig. 1, the LCFBG is employed to implement the wavelength-to-time mapping. Assuming the value of the dispersion of the LCFBG is $\ddot{\Phi}$ (ps/nm), for an input light pulse $g(t)$, the reflected light wave at the 3rd port of OC2 is given by [10]

$$y(t) = \exp\left(j\frac{\lambda^2}{c} \times \frac{t^2}{2\ddot{\Phi}_v}\right) \times G(\omega)\Big|_{\omega = \frac{t}{\ddot{\Phi}_v}} \qquad (2)$$

where $G(\omega)$ is the Fourier transform of $g(t)$, and the dispersion $\ddot{\Phi}_v$ (ps^2) is calculated by $\ddot{\Phi}_v = \frac{\lambda^2}{c}\ddot{\Phi}$.

From (2), it can be seen that the envelope of the reflected light wave is proportional to the Fourier transform of the input light wave, which is the spectrum of the random grating. By applying the reflected optical pulse to a PD, an electrical random waveform is obtained. When a strain or temperature change is applied to the random grating, the wavelength shift will be translated to a temporal shift, given by

$$\Delta\tau = \ddot{\Phi}\Delta\lambda \qquad (3)$$

where $\Delta\tau$ is the temporal shift and $\Delta\lambda$ is the wavelength shift.

For a HBRG, the refractive indices of the fast axis and slow axis are different because of the birefringence of the fiber. Then, (1) can be rewritten as

$$\begin{bmatrix} \Delta\lambda_f \\ \Delta\lambda_s \end{bmatrix} = \begin{bmatrix} g_{f1} & g_{f2} \\ g_{s1} & g_{s2} \end{bmatrix}\begin{bmatrix} \Delta\varepsilon \\ \Delta T \end{bmatrix} \qquad (4)$$

where g_{f1}, g_{f2} and g_{s1}, g_{s2} are the coefficients for the fast axis and slow axis, respectively, and $\Delta\lambda_f$, $\Delta\lambda_s$ are the wavelength shifts along the fast and slow axes, respectively.

The relationship between the wavelength shifts and the strain and temperature is given by

$$\begin{bmatrix} \Delta\varepsilon \\ \Delta T \end{bmatrix} = \begin{bmatrix} g_{f1} & g_{f2} \\ g_{s1} & g_{s2} \end{bmatrix}^{-1}\begin{bmatrix} \Delta\lambda_f \\ \Delta\lambda_s \end{bmatrix} \qquad (5)$$

As shown in Fig. 1, an optical pulse entering the optical loop will be split into two orthogonally polarized pulses, and the two pulses will experience complementary dispersion introduced by the LCFBG. Thus, (3) can be rewritten as

$$\begin{bmatrix} \Delta\tau_x \\ \Delta\tau_y \end{bmatrix} = \ddot{\Phi}\begin{bmatrix} \Delta\lambda_f \\ -\Delta\lambda_s \end{bmatrix} \qquad (6)$$

where $\Delta\tau_x$ and $\Delta\tau_y$ are the time shifts of the correlation peaks for the horizontally and vertically polarized pulses, respectively.

Substitute (6) into (5), we get

$$\begin{bmatrix} \Delta\varepsilon \\ \Delta T \end{bmatrix} = \frac{1}{\ddot{\Phi}}\begin{bmatrix} g_{f1} & g_{f2} \\ g_{s1} & g_{s2} \end{bmatrix}^{-1}\begin{bmatrix} \Delta\tau_x \\ -\Delta\tau_y \end{bmatrix} \qquad (7)$$

As can be seen, the strain and the temperature information can be measured by measuring the time shifts of the correlation peaks of the horizontally and vertically polarized pulses.
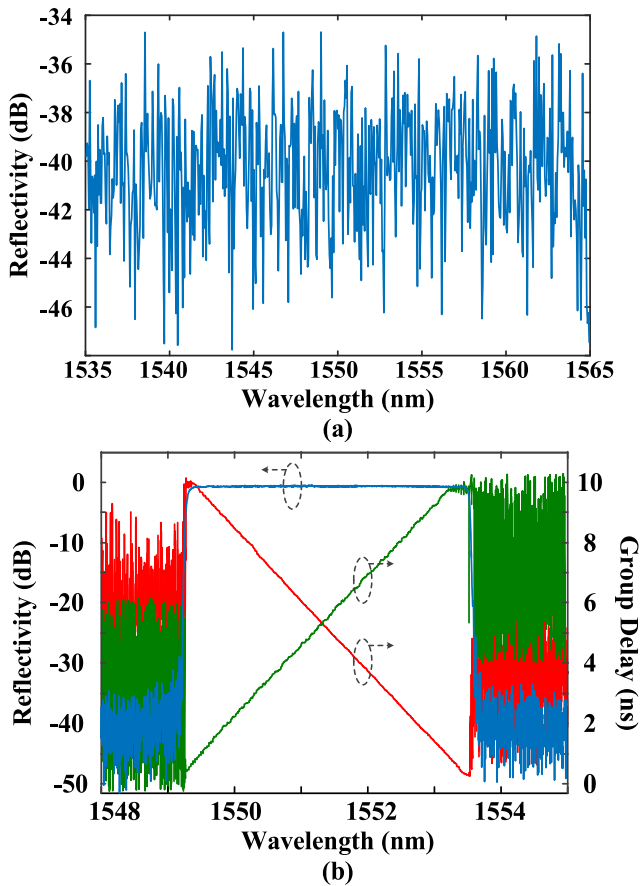
Fig. 3. (a) Reflection spectrum of the fabricated HBRG; (b) Reflection spectrum and group delay response of the LCFBG.
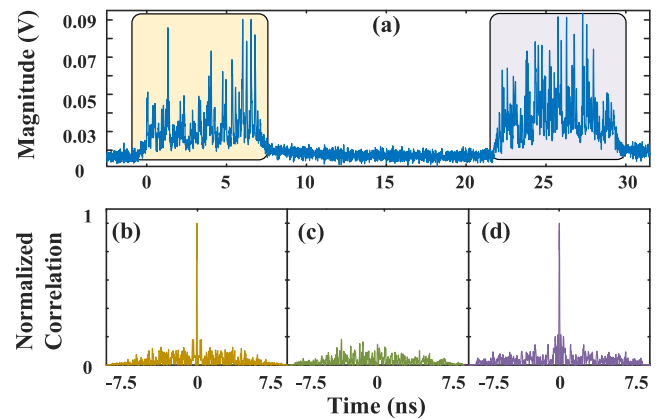

Fig. 4. (a) Generated random waveforms; (b) auto-correlation of the waveform from the horizontal direction; (c) cross-correlation between the waveforms from the two directions; (d) auto-correlation of the waveform from the vertical direction.

III. EXPERIMENTAL RESULTS

An experiment based on the setup shown in Fig. 1 is performed. An ultrashort light pulse train with a repetition rate of 20 MHz generated by a tunable MLL (PriTel FFL-1550-20) with a 3-dB bandwidth of 8 nm and a pulse width of less than 600 fs is applied to a HBRG via a programmable bandpass optical filter (Waveshaper 4000S) and OC1. The random grating is fabricated in a polarization maintaining fiber (PMF) with a length of 50 mm. The reflection spectrum of the random grating is measured by a joint use of a tunable laser source (Yokogawa AQ2201) and an optical spectrum analyzer (Ando AQ6312B), as shown in Fig. 3(a). As can be seen, the random reflection spectrum over 30 nm is obtained.

Then an optical pulse reflected from the HBRG is sent to the optical loop, where the horizontally polarized optical pulse is directed by the PBS to the left path, and the vertically polarized optical pulse is directed to the right path. The optical pulses are then experiencing wavelength-to-time mapping at the LCFBG. The LCFBG used in the experiment is fabricated in a single-mode fiber (SMF) with a length of 1 m. Its reflection spectrum is measured by an optical vector analyzer (OVA, Luna Technologies) and is shown in Fig. 3(b). As can be seen, the LCFBG has a bandwidth of 4 nm and a central wavelength of 1551.4 nm. The group delay responses measured from its short and long wavelength ends are also shown in Fig. 3(b). It can be seen that two

group delay responses are complementary and the dispersion coefficients are $+2500$ ps/nm and -2500 ps/nm, respectively. The central wavelength of the ultrashort light pulse is tuned at 1551.4 nm, which is identical to the central wavelength of the LCFBG, and the bandwidth of the optical filter is set as 3 nm, to get a higher optical power density for effective photodetection. Thus, the pulse width of the generated waveform should be 7.5 ns. The repetition rate of the pulse train is 20 MHz. To avoid overlap between two adjacent pulses, the time delay introduced by the delay line in the optical loop should be greater than 7.5 ns and smaller than 35 ns.

After amplified by an EDFA, the optical pulses after wavelength-to-time mapping are fed into a PD (Newport, model 1014, 45 GHz) and the generated electrical waveforms are monitored by a real-time oscilloscope (Keysight, DSOZ504A, 50 GHz bandwidth, 160 GSa/s). Fig. 4(a) shows the generated electrical waveforms, from which we could see that the pulse widths are around 7.5 ns. Fig. 4(b), (c) and (d) shows the auto-correlation of the waveform from the horizontal polarization direction, cross-correlation between the waveforms from the two directions, and the auto-correlation of the waveform from the vertical polarization direction, respectively. As can be seen, the pulses are significantly compressed for auto-correlation, and no correlation peak is observed for cross-correlation. The results confirm that a random waveform can be significantly compressed for autocorrelation, and no compressed pulse is obtained for cross-correlation since the two waveforms used for cross-correlation are different due to the complementary wavelength-to-time mapping.

Fig. 5 shows the compressed pulses from the horizontal direction when a different temperature is applied to the HBRG sensor while maintaining the strain constant. The reference waveform is one generated at 82 °C. As can be seen, the height of the cross-correlation peak is reducing when the temperature applied to the HBRG is decreasing. This is because the overlap regions between the measured random waveform and the reference random waveform are reducing when the temperature is decreasing, leading to a reduced cross-correlation peak. If the
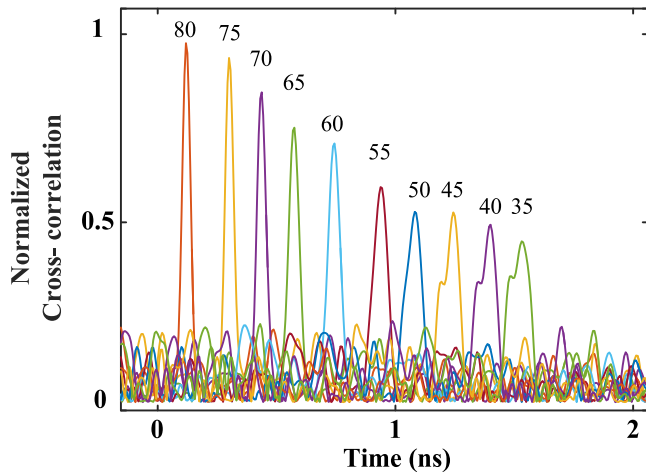
Fig. 5. Compressed pulses from the horizontal direction when different temperatures are applied to the HBRG sensor.
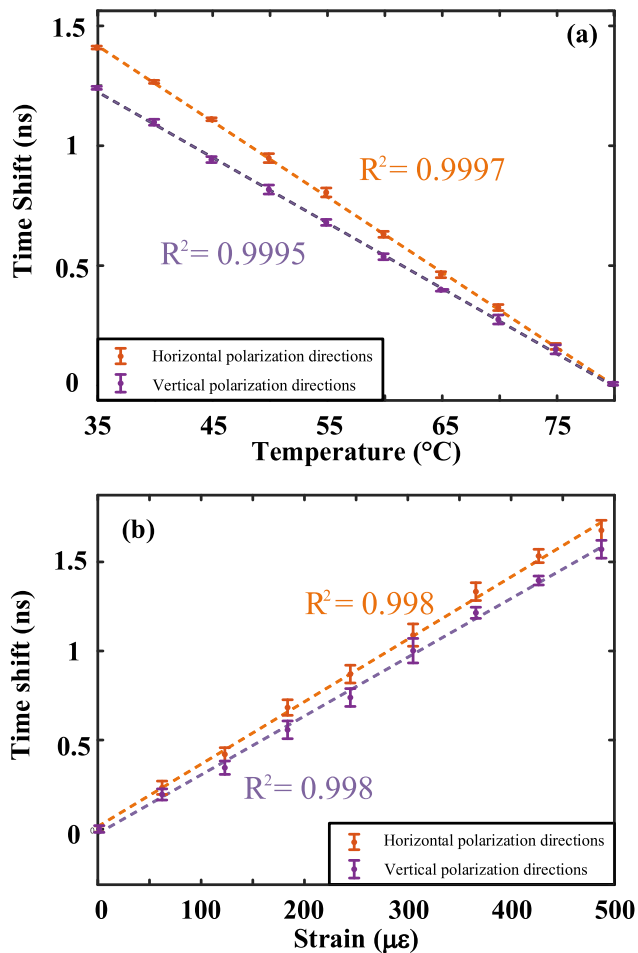

Fig. 6. (a) Time shifts versus temperature changes with no strain applied; (b) Time shifts versus strain changes at a fixed room temperature (23.2 °C).

length of the random waveform is much longer than the time shift due to a strain or temperature change, the reduction in the cross-correlation peak will be small and negligible.

Fig. 6(a) shows the time shifts of the compressed pulses versus temperature change with no strain applied, and Fig. 6(b) shows the time shifts of the compressed pulses versus strain change at a fixed room temperature (23.2 °C). Based on the measurements in Fig. 6, we get the relationship between the strain and temperature and the time shifts,

$$
\begin{bmatrix} \Delta\varepsilon \\ \Delta T \end{bmatrix} = \begin{bmatrix} 0.398\ \mu\varepsilon/\text{ps} & -0.422\ \mu\varepsilon/\text{ps} \\ -3.291\ °\text{C/ps} & 3.793\ °\text{C/ps} \end{bmatrix} \begin{bmatrix} \Delta\tau_x \\ -\Delta\tau_y \end{bmatrix} \quad (8)
$$

As can be seen, for this system, once the temporal shifts are measured, the strain and temperate information can be retrieved simultaneously.

Based on Fig. 6, the sensitivities are calculated to be 31.48 ps/°C and 3.5 ps/$\mu\varepsilon$, which can be further improved if an LCFBG with a greater dispersion coefficient is used. The minimum width of the compressed pulses is 25 ps, corresponding to a temperature resolution of 0.79 °C and strain resolution of 7.1 $\mu\varepsilon$, which can be improved if a PD with a wider bandwidth, an LCFBG with a greater dispersion, and a random grating with a higher randomness are employed. The minimum detectable wavelength shift is determined by the sampling rate of the oscilloscope and the dispersion coefficient of the LCFBG. The sampling rate of the oscilloscope is 160 GSa/s, and the dispersion coefficient of the LCFBG is 2500 ps/nm, so the minimum detectable wavelength shift is calculated to be 2.5 pm. The interrogation speed is determined by the repetition rate of the MLL, which is 20 MHz. The experimental errors are within ±0.8 °C and ±9 $\mu\varepsilon$. Comparing with the results reported in [15], [21], this system shows a higher sensitivity and higher accuracy. Without using an interferometric structure, the system is ultra-stable.

IV. CONCLUSION

We have proposed and experimentally demonstrated a new approach to achieve high-speed and high-resolution interrogation of a HBRG sensor based on spectral shaping and wavelength-to-time mapping and pulse compression for simultaneous measurement of strain and temperature. The key contribution of the work was the use of a HBRG to generate a random spectrum, which was compressed in the time domain after wavelength-to-time mapping. Since the spectrums were converted to the time domain, high speed and high resolution integration using a DSP is possible. In addition, pulse compression enabled the interrogation with an increased resolution. The approach was verified experimentally. Simultaneous measurements of strain and temperature with a resolution of 7.1 $\mu\varepsilon$ and 0.79 °C at an ultra-high speed of 20 MHz were demonstrated.

REFERENCES

[1] S. Yin, P. Ruffin, and F. Yu. *Fiber Optic Sensors*, 2nd ed. Boca Raton, FL, USA: CRC Press, 2008.
[2] A. D. Kersey *et al.*, "Fiber grating sensors," *J. Lightw. Technol.*, vol. 15, no. 8, pp. 1442–1463, Aug. 1997.
[3] S. M. Topliss, S. W. James, F. Davis, S. P. Higson, and R. P. Tatam, "Optical fibre long period grating based selective vapour sensing of volatile organic compounds," *Sens. Actuator B-Chem.*, vol. 143, no. 2, pp. 629–634, Oct. 2009.
[4] J. Yao, "Microwave photonics for high resolution and high speed interrogation of fiber Bragg grating sensors," *Fiber Integr. Opt.*, vol. 34, no. 4, pp. 230–242, Oct. 2015.

[5] C. G. Askins, M. A. Putnam, G. M. Williams, and E. J. Friebele, "Stepped-wavelength optical fiber Bragg grating arrays fabricated in line on a draw tower," *Opt. Lett.*, vol. 19, no. 2, pp. 147–149, Jan. 1994.

[6] Q. Zhang *et al.*, "Use of highly overcoupled couplers to detect shifts in Bragg wavelength," *Electron. Lett.*, vol. 31, no. 6, pp. 480–482, Mar. 1995.

[7] H. Xia, C. Zhang, H. Mu, and D. Sun, "Edge technique for direct detection of strain and temperature based on optical time domain reflectometry," *Appl. Opt.*, vol. 48, no. 2, pp. 189–197, Jan. 2009.

[8] Y. J. Rao, D. A. Jackson, L. Zhang, and I. Bennion, "Dual-cavity interferometric wavelength-shift detection for in-fiber Bragg grating sensors," *Opt. Lett.*, vol. 21, no. 19, pp. 1556–1558, Oct. 1996.

[9] C. Wang and J. Yao, "Ultrafast and ultrahigh-resolution interrogation of a fiber Bragg grating sensor based on interferometric temporal spectroscopy," *J. Lightw. Technol.*, vol. 29, no. 19, pp. 2927–2933, Oct. 2011.

[10] J. Yao, "Photonic generation of microwave arbitrary waveforms," *Opt. Comm.*, vol. 284, no. 15, pp. 3723–3736, Jul. 2011.

[11] Y. Dai, J. Li, Z. Zhang, F. Yin, W. Li, and K. Xu, "Real-time frequency-to-time mapping based on spectrally-discrete chromatic dispersion," *Opt. Express*, vol. 25, no. 14, pp. 16660–16671, May 2017.

[12] V. Torres-Company, D. E. Leaird, and A. M. Weiner, "Dispersion requirements in coherent frequency-to-time mapping," *Opt. Express*, vol. 19, no. 24, pp. 24718–24729 Sep. 2011.

[13] W. Liu, M. Li, C. Wang, and J. Yao, "Real-time interrogation of a linearly chirped fiber Bragg grating sensor with improved resolution and signal-to-noise ratio," *J. Lightw. Technol.*, vol. 29, no. 9, pp. 1239–1247, May 2011.

[14] O. Xu, J. Zhang, and J. Yao, "High speed and high resolution interrogation of a fiber Bragg grating sensor based on microwave photonic filtering and chirped microwave pulse compression," *Opt. Lett.*, vol. 41, no. 21, pp. 4859–4862, Nov. 2016.

[15] Y. Wang, J. Zhang, O. L. Coutinho, and J. Yao, "Interrogation of a linearly chirped fiber Bragg grating sensor with a high resolution using a linearly chirped optical waveform," *Opt. Lett.*, vol. 40, no. 21, pp. 4923–4926, Nov. 2015.

[16] Y. Wang, J. Zhang, and J. Yao, "An optoelectronic oscillator for high sensitivity temperature sensing," *IEEE Photon. Technol. Lett.*, vol. 28, no. 13, pp 1458–1460, Jul. 2016.

[17] J. Yao, "Optoelectronic oscillators for high speed and high resolution optical sensing," *J. Lightw. Technol.*, vol. 35, no. 16, pp. 3489–3497, Aug. 2017.

[18] P. Lu *et al.*, "Plane-by-plane inscription of grating structures in optical fibers," *J. Lightw. Technol.*, vol. 36, no. 4, pp. 926–931, Sep. 2017.

[19] Y. Xu, P. Lu, S. Gao, D. Xiang, S. Mihailov, and X. Bao, "Optical fiber random grating-based multiparameter sensor," *Opt. Lett.*, vol. 40, no. 23, pp. 5514–5517, Dec. 2015.

[20] M. A. Herman, and T. Strohmer, "High-resolution radar via compressed sensing," *IEEE Trans. Signal Process.*, vol. 57, no. 6, pp. 2275–2284, Jun. 2009.

[21] L. Meng, W. Zou, X. Li, and J. Chen. "Ultrafast FBG interrogator based on time-stretch method," *IEEE Photon. Technol. Lett.*, vol. 28, no. 7, pp. 778–781, Apr. 2016.

Hong Deng (S'16) received the B.Eng. degree in optoelectronic information engineering from Huazhong University of Science and Technology, Wuhan, China, in 2014 and the Master's degree in applied science from the Microwave Photonics Research Laboratory, School of Electrical Engineering and Computer Science, University of Ottawa, Ottawa, ON, Canada, in 2018. He is currently working toward the Ph.D. degree in electrical engineering at the Photonics Research Group, Department of Information Technology, IMEC, Ghent University, Ghent, Belgium.

His current research interests include large programmable photonic integrated circuits, silicon photonics, and microwave photonics.

Ping Lu received the B.Sc. and M.Sc. degrees from Jilin University, Changchun, China, in 1988 and 1991, respectively, and the Ph.D. degree from the University of Ottawa, Ottawa, ON, Canada, in 2002, all in physics. From 1991 to 1997, he was a Lecturer with Jilin University, where his research focused on the fabrication and application of infrared fibers. Since 2002, he has been a Research Scientist with the Optical Communications and Electrophotonics Group, Communications Research Centre Canada, Ottawa.

His current research interests are mainly in the study of polarization effects in fiber-optic communication systems and fiber Bragg gratings.

Stephen J. Mihailov (M'96) received the B.Sc. degree in physics from Carleton University, Ottawa, ON, Canada, in 1986 and the Ph.D. degree in physics from York University, Toronto, ON, Canada, in 1992. Between 1994 and 1996, he was with JDS-Fitel Incorporated, Nepean, ON, Canada, where he worked on the development of passive optical component technology and was the Project Leader for the development of fiber Bragg grating technology. In 1996, he joined the Optical Communications and Electrophotonics group of the Communications Research Centre Canada as a Research Scientist, where he conducted research on network applications of fiber Bragg gratings. He is currently the Research Program Manager of the Optical Communications and Electrophotonics group at the Communications Research Centre. He was a Natural Sciences and Engineering Research Council of Canada (NSERC) Postdoctoral Fellow from 1992 to 1994 where he conducted research on laser-material processing of polymers and glasses at the L'Université de Bordeaux I, Bordeaux, France, and at Exitech Ltd., Oxford, U.K.

Jianping Yao (M'99–SM'01–F'12) received the Ph.D. degree in electrical engineering from the Université de Toulon et du Var, Toulon, France, in December 1997. He is a Distinguished University Professor and University Research Chair with the School of Electrical Engineering and Computer Science, University of Ottawa, Ottawa, ON, Canada. From 1998 to 2001, he was with the School of Electrical and Electronic Engineering, Nanyang Technological University, Singapore, as an Assistant Professor. In December 2001, he joined the School of Electrical Engineering and Computer Science, University of Ottawa as an Assistant Professor, where he was promoted to Associate Professor in May 2003, and a Full Professor in May 2006. He was appointed the University Research Chair in Microwave Photonics in 2007. In June 2016, he was conferred the title of Distinguished University Professor of the University of Ottawa. From July 2007 to June 2010 and from July 2013 to June 2016, he was the Director of the Ottawa-Carleton Institute for Electrical and Computer Engineering. He has authored or co-authored more than 560 research papers including more than 330 papers in peer-reviewed journals and more than 230 papers in conference proceedings.

Prof. Yao is the Editor-in-Chief of IEEE PHOTONICS TECHNOLOGY LETTERS, a Topical Editor of *Optics Letters*, an Associate Editor of *Science Bulletin*, a Steering Committee Member of the IEEE JOURNAL OF LIGHTWAVE TECHNOLOGY, and an Advisory Editorial Board Member of *Optics Communications*. He was a Guest Editor of a Focus Issue on Microwave Photonics in *Optics Express* in 2013, a Lead-Editor of a Feature Issue on Microwave Photonics in *Photonics Research* in 2014, and a Guest Editor of a Special Issue on Microwave Photonics in the IEEE JOURNAL OF LIGHTWAVE TECHNOLOGY in 2018. He is currently the Chair of the IEEE Photonics Ottawa Chapter and is the Technical Committee Chair of IEEE MTT-3 Microwave Photonics. He was a member of the European Research Council Consolidator Grant Panel in 2016, the Qualitative Evaluation Panel in 2017, and a member of the National Science Foundation Career Awards Panel in 2016. He was also a chair of a number of international conferences, symposia, and workshops, including the Vice Technical Program Committee (TPC) Chair of the 2007 IEEE Topical Meeting on Microwave Photonics, TPC Co-Chair of the 2009 and 2010 Asia-Pacific Microwave Photonics Conference, TPC Chair of the High-Speed and Broadband Wireless Technologies Subcommittee of the IEEE Radio Wireless Symposium 2009-2012, TPC Chair of the Microwave Photonics Subcommittee of the IEEE Photonics Society Annual Meeting 2009, TPC Chair of the 2010 IEEE Topical Meeting on Microwave Photonics, General Co-Chair of the 2011 IEEE Topical Meeting on Microwave Photonics, TPC Co-Chair of the 2014 IEEE Topical Meetings on Microwave Photonics, and General Co-Chair of the 2015 and 2017 IEEE Topical Meeting on Microwave Photonics. He was also a committee member for a number of international conferences, such as IPC, OFC, BGPP, and MWP. He is the recipient of the 2005 International Creative Research Award of the University of Ottawa, the 2007 George S. Glinski Award for Excellence in Research, a Natural Sciences and Engineering Research Council of Canada Discovery Accelerator Supplements Award in 2008, an inaugural OSA Outstanding Reviewer Award in 2012, and the Award for Excellence in Research 2017-2018 of the University of Ottawa. He was one of the top ten reviewers of IEEE/OSA JOURNAL OF LIGHTWAVE TECHNOLOGY (2015–2016). He was an IEEE MTT-S Distinguished Microwave Lecturer for 2013–2015. He is a registered Professional Engineer of Ontario. He is a Fellow of the Optical Society of America, the Canadian Academy of Engineering, and the Royal Society of Canada.